

1 **The anti-proliferative effect of cation channel blockers in T lymphocytes depends on the**
2 **strength of mitogenic stimulation**

3 Authors: Zoltan Petho¹, Andras Balajthy¹, Adam Bartok¹, Krisztian Bene², Sandor Somodi³,
4 Orsolya Szilagyi¹, Eva Rajnavolgyi², Gyorgy Panyi¹, Zoltan Varga^{1,4}

5 Affiliation:

- 6 1) Department of Biophysics and Cell Biology, Faculty of General Medicine, University
7 of Debrecen, Debrecen, Hungary
8 2) Department of Immunology, Faculty of General Medicine, University of Debrecen,
9 Debrecen, Hungary
10 3) 1st Department of Internal Medicine, University of Debrecen, Debrecen, Hungary
11 4) MTA-DE-NAP B Ion Channel Structure-Function Research Group, RCMM,
12 University of Debrecen, Debrecen, Egyetem tér 1, H-4032, Hungary
13

14 **Keywords:** Immune regulation; T cells; Cellular proliferation; Cytokine secretion; Ion channel;
15 Rapamycin

16

17 **Name of the correspondent author:** Gyorgy Panyi, M.D., Ph.D., D.Sc.

18 **Postal Address:** Nagyerdei krt. 98, H-4032 Debrecen, Hungary

19 **Telephone:** (+36)(52) 412-623

Fax: (+36)(52)532-201

20 **E-mail address:** panyi@med.unideb.hu

21 **List of abbreviations:**

22 CRAC: Ca²⁺-release activated Ca²⁺ channel

23 CD: Cluster of differentiation

24 PI: Propidium iodide

25 mTOR: Mammalian target of rapamycin

26 FKBP: FK506 binding protein

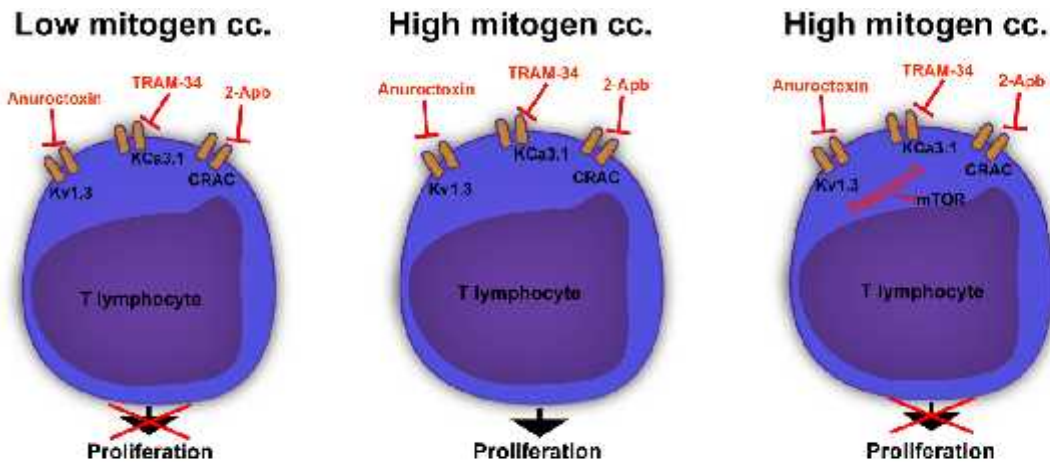
27 Antx: Anuroctoxin

28 2-Apb: 2-Aminoethoxydiphenyl borate

29 DI: Division index

30 PBMC: Peripheral blood mononuclear cell

31 CFSE: Carboxifluorescein succinimidyl ester



33 Ion channel blockers inhibit T lymphocyte proliferation at low mitogen concentrations. This
 34 effect diminishes upon using higher mitogen concentrations, but the antiproliferative effect can
 35 be recovered by combining ion channel blockers with other immunopharmacological agents such
 36 as the mTOR inhibitor rapamycin.

37

Abstract

38 Ion channels are crucially important for the activation and proliferation of T lymphocytes,
 39 and thus, for the function of the immune system. Previous studies on the effects of channel
 40 blockers on T cell proliferation reported variable effectiveness due to differing experimental
 41 systems. Therefore our aim was to investigate how the strength of the mitogenic stimulation
 42 influences the efficiency of cation channel blockers in inhibiting activation, cytokine secretion
 43 and proliferation of T cells under standardized conditions.

44 Human peripheral blood lymphocytes were activated via monoclonal antibodies targeting
 45 the TCR-CD3 complex and the co-stimulator CD28. We applied the blockers of Kv1.3
 46 (Anuroctoxin), KCa3.1 (TRAM-34) and CRAC (2-Apb) channels of T cells either alone or in
 47 combination with rapamycin, the inhibitor of the mammalian target of rapamycin (mTOR). Five

48 days after the stimulation ELISA and flow cytometric measurements were performed to
49 determine IL-10 and IFN- secretion, cellular viability and proliferation.

50 Our results showed that ion channel blockers and rapamycin inhibit IL-10 and IFN-
51 secretion and cell division in a dose-dependent manner. Simultaneous application of the blockers
52 for each channel along with rapamycin was the most effective, indicating synergy among the
53 various activation pathways. Upon increasing the extent of mitogenic stimulation the anti-
54 proliferative effect of the ion channel blockers diminished. This phenomenon was unknown to
55 date but may be important in understanding the fine-tuning of T cell activation.

56 *1. Introduction*

57 T lymphocytes are highly potent cells of the adaptive immune system and are crucially
58 important in the maintenance of immunological homeostasis. Rapid and specific activation
59 through the TCR and its co-receptors CD4 and/or CD8 lead to the recruitment of numerous down-
60 stream pathways, that ultimately result in T cell activation and proliferation, and subsequently
61 lead to the differentiation into effector or memory cells [1,2].

62 Physiological T cell activation occurs upon contact with professional antigen presenting
63 cells. The consequence of antigen presentation depends on the age and the stage of differentiation
64 of the T cell, and also on the intensity and the duration of the stimulus [3]. It is well established
65 that the co-localization of different signaling molecules forms an immunological synapse, which
66 enhances the subsequent cellular response [4,5]. The molecules forming the immunological
67 synapse on the T cell side involve the TCR-CD3 complex together with co-activator molecules
68 such as CD28 [6], CD40 ligand [7] or the IL-2R [8].

69 Considering that the underlying mechanisms of lymphocyte stimulation are necessary for
70 understanding the ensuing immune responses, various methods were designed to mimic *in vivo*
71 activation pathways. These methods include monoclonal antibodies targeting the TCR-CD3

72 complex and other co-activator molecules [9,10]; cross linking of cell surface glycoproteins via
73 mitogenic lectins such as PHA [11] and bypassing T cell Ca^{2+} -signaling by ionomycin and the
74 diacylglycerol-analog PMA [12]. As these methods are not epitope-specific, they result in a high
75 degree of cytokine secretion, such as the anti-inflammatory cytokine IL-10 and the inflammatory
76 cytokine IFN- γ , and eventually in T cell activation and mitosis [13]. The pro-inflammatory IFN- γ
77 is secreted by a wide array of cells, such as natural killer cells, Th₁ CD4 and CD8 cytotoxic T
78 cells and even macrophages. On the other hand, anti-inflammatory IL-10 is mainly secreted by
79 Th₂ T cells and regulatory CD4⁺/CD25⁺/FoxP3⁺ T_{reg} cells [14].

80 Ion channels are important in cellular signaling, even in electrically non-excitabile cells,
81 such as immune cells. Since 1984, when electric signals from lymphocytes were first recorded
82 [15,16], it has been suggested that ion channels are involved in the regulation of the immune
83 system. To date numerous ion channels have been discovered in T cells (summarized in [17,18]):
84 the Ca^{2+} -release activated Ca^{2+} channel (CRAC) [19]; the Shaker-type voltage-gated K^+ channel
85 Kv1.3 [20], the Ca^{2+} -activated K^+ channel, KCa3.1, formerly known as IKCa1 [21,22]; the non-
86 selective TRPM7, that is suggested to be involved in the magnesium homeostasis of the cell;
87 TRPM2, important in T cell activation and proliferation [23], and finally the swelling-activated
88 chloride channel Cl_{swell} , encoded by the SWELL 1 gene [14,24]. As CRAC, Kv1.3 and KCa3.1
89 channels co-localize in the immune synapse and are up-regulated in different T-cell subtypes
90 [5,25], it is widely accepted that these channels are indispensable early factors in the Ca^{2+} -
91 dependent activation pathways of the T cell [26]. Increase in $[\text{Ca}]_i$ may activate pathways
92 involving the calcium-calmodulin complex and other secondary messenger molecules such as
93 calcineurin. This phosphatase dephosphorylates the nuclear factor of activated T-cells (NFAT),
94 allowing its dimerization and nuclear translocation. This transcription factor can then bind to the
95 promoter region of target genes involved in cytokine production and proliferation of T
96 lymphocytes [20,26].

97 As ion channels are key players in T lymphocyte activation, their blockade can decrease
98 the array of pathological immune responses *in vivo*. Kv1.3 is an excellent candidate for
99 immunotherapy, as it is expressed predominantly in astrocytes, T lymphocytes and
100 oligodendrocytes [27] in contrast to CRAC and KCa3.1 channels, that are widely distributed and
101 thus their blockers may have more side effects. Successful experimental trials employing Kv1.3
102 blockers have already been performed in animal models of autoimmune diseases such as multiple
103 sclerosis [25], type 1 diabetes mellitus or rheumatoid arthritis [28].

104 Besides the Ca²⁺-dependent mechanisms, other signaling pathways also participate in T
105 cell activation that do not involve NFAT signaling. Such pathways include the mammalian target
106 of rapamycin (mTOR), which contributes to the activation of both translational and metabolic
107 pathways, and allows DNA synthesis [29,30]. The mTOR can be blocked indirectly using
108 rapamycin (also known as sirolimus), which inhibits the FK506 binding protein (FKBP12), that
109 interacts with mTOR. Rapamycin is a highly effective immunosuppressive drug, that is currently
110 widely used in the treatment of kidney graft rejection or graft versus host disease [31].

111 The anti-proliferative effects of different ion channel blockers on T cells have already
112 been described in a number of experiments and reviews. However, there is an obvious variability
113 in the results of previous studies related to this topic. For example, the average blocker
114 concentration necessary for 50% inhibition of cell proliferation ranged from 1×K_d concentration
115 to 1000×K_d in case of Kv1.3 channel blockers, or from 1.5×K_d to 275 × K_d in the case of the
116 KCa3.1-blocker TRAM-34, where K_d is the drug concentration required to block half of the
117 relevant channels [25,32-35]. Moreover, TRAM-34 inhibition alone had no effect on the
118 proliferation of mixed T cell populations [36]. The underlying mechanism responsible for this
119 variability has not been systematically addressed before, but must be largely due to the different
120 methods of T cell stimulation and different doses of mitogens applied in these studies. Therefore
121 our aim was to elucidate this phenomenon by comparing the anti-proliferative effects of ion

122 channel blockers and rapamycin on lymphocytes cultured and activated under identical
123 experimental conditions. Moreover, considering our results at various mitogen concentrations,
124 we propose a theory to explain the underlying mechanisms of our observations.

125

126

2. Materials and Methods

127

2.1 Isolation and cultivation of mononuclear cells

128 PBMCs were isolated from heparinized (heparin from TEVA Pharmaceutical Industries
129 Ltd., Debrecen, Hungary) peripheral blood of healthy volunteers. First the blood was diluted with
130 Hanks' Balanced Salt Solution (HBSS; from Sigma-Aldrich Co., Saint Louis, MO, USA) in 1:1
131 ratio, and then centrifuged using the Ficoll-Hypaque density gradient (GE Healthcare Life
132 Sciences, Little Chalfont, UK) at 1400 rpm for 30 minutes at room temperature. Next, the opaque
133 layer of mononuclear cells was collected and washed two times with 50 ml HBSS. In n=4
134 experiments we used purified CD3⁺ T lymphocytes obtained by negative selection using
135 RosetteSep™ (Stem Cell Technologies™, Vancouver, Canada) technique according to the
136 description in the manual. We did not find significant differences between CD3⁺ T cells and
137 PBMCs regarding the extent of proliferation (p=0.785) or in the proliferation-inhibiting effect of
138 Antx at K_d (p=0.667) and 10K_d (p=0.333) concentrations. Therefore, we used the PBMC
139 population in the majority of our experiments.

140 Following carboxyfluorescein succinimidyl ester staining (CFSE stining, see below) and
141 activation, cells were cultured in 24 or 96 well plates at a cell density of 10⁶ cells/ml in standard
142 RPMI-1640 medium (Sigma-Aldrich Co., Saint Louis, MO, USA) containing 15% HEPES buffer
143 (Sigma-Aldrich Co., Saint Louis, MO, USA) at 37°C in humid atmosphere with 5% CO₂. In
144 every experiment all plates were incubated for 5 days and were supplemented with fresh culture

145 medium on day 3. After harvesting, the cells underwent propidium iodide (PI) staining and
146 subsequent FACS analysis.

147

148 **2.2 CFSE dilution assay and PI staining**

149 We applied the CFSE dilution assay, originally described by Lyons et al [37-39], to
150 measure the rate of proliferation. The staining procedure briefly was the following: the
151 membrane-permeable, but non-fluorescent carboxyfluorescein diacetate succinimidyl ester
152 (CFDA-SE) binds to structural proteins within the cell, and is subsequently cleaved by
153 nonspecific esterases to become the membrane non-permeable and fluorescent molecule CFSE.
154 Upon cell division, the amount of CFSE is gradually halved in the daughter cells, thus the number
155 of division cycles the cells have undergone can be determined. In our case, the lymphocytes
156 divided usually every 24-48 hours, leading to 4-6 measurable cycles at the end of our
157 experiments.

158 The final concentration of CFDA-SE (CellTrace™ CFSE Cell Proliferation Kit, Life
159 Technologies Co., Waltham, MA, USA) in our experiments was 1 μ M that provided a 100-to-
160 1000-fold increase in the fluorescence intensity of the measured cells over the autofluorescence
161 of unstained cells. After adding CFDA-SE, we incubated the PBMCs or T lymphocytes for 15
162 min at room temperature, then for 20 min at 37°C. Lastly, the cells were washed once with
163 phosphate buffer solution (PBS). We took care that the CFSE-stained cells remained hidden from
164 excess light during our experiments. This CFSE staining can be ultimately recorded by flow
165 cytometry.

166 PI staining was performed at the end of the 5-day incubation period. Therefore, we
167 harvested and washed the cells once using HBSS, then added 1 μ l PI to the cell suspension. Cells

168 were mixed gently with PI and then incubated in the dark for 5 minutes at room temperature. The
169 flow cytometer settings were adjusted to a negative control tube containing unstained cells. PI
170 fluorescence intensity was measured in the red channel, because samples were co-stained with
171 CFSE.

172 **2.3 Selective stimulation of T lymphocytes**

173 At the beginning of the present study, we performed preliminary experiments regarding
174 our preferred method of stimulation. Four widely used and well-known lymphocyte stimulation
175 techniques were compared using CFSE dilution assay on PBMCs: PHA stimulation [11]; PMA
176 combined with ionomycin [12]; soluble anti-CD3 antibody alone and in combination with anti-
177 CD28 [9,10]. Moreover, we measured whole-cell K^+ currents and current density on
178 representative populations of the stimulated T cells. We found the anti-CD3 and anti-CD28
179 stimulation was most reproducible (data not shown) and thus, we used this approach in our
180 experiments detailed in this article.

181 We applied 200 nM – 3 μ M soluble anti-CD3 antibodies combined with a constant
182 amount of 1 μ g/ml soluble mouse anti-human CD28 (Sigma-Aldrich Co., Saint Louis, MO, USA)
183 in n=8 experiments for specific T cell stimulation in the PBMC and lymphocyte cultures. We
184 enhanced the rate of stimulation by adding the soluble antibodies to the bottom of the culture
185 well, left it to bind to the plate surface for 30 minutes at room temperature, then cells were added
186 to the wells in culture medium suspension. In n=8 experiments we used superparamagnetic bead-
187 conjugated anti-CD3 and anti-CD28 monoclonal antibodies (Life Technologies Co., Waltham,
188 MA, USA), which we found more user-friendly than the soluble antibodies. The pairwise
189 comparison of soluble mitogens and bead-mediated stimulation Student's t-test showed no
190 significant difference between the divided cell populations with the two methods of stimulation
191 ($p=0.336$). The beads are also known to provide adequate cross-linking thus inducing a relatively

192 high level of activation [10], in contrast to stimulation with soluble anti-CD3 and anti-CD28, that
193 resulted in a higher amount of variability in our measurements [9]. The bead:cell ratio in these
194 cases was 1:200 - 1:1 (see Results).

195

196 **2.4 Application of ion channel blockers and rapamycin**

197 To block the Kv1.3 channel we used the peptide-type toxin Antx [40]. KCa3.1 channels
198 in were blocked using TRAM-34 (Sigma-Aldrich Co., Saint Louis, MO, USA) [34] and the
199 CRAC channels were inhibited by 2-Apb (Sigma-Aldrich Co., Saint Louis, MO, USA) [41]. We
200 used the ion channel blockers at two concentrations: the lower was equal to the dissociation
201 constant, or $1 \times K_d$, of ion channel inhibition of the blockers and the higher was 10 times the K_d
202 ($10 \times K_d$). In the case of Antx, we used 500 pM ($1 \times K_d$) and 5 nM [40]. In the case of 2-Apb the
203 K_d for lymphocytes is 5 μ M, and the other concentration used was 50 μ M. Finally, the KCa3.1
204 blocker TRAM-34 was used in 20 nM ($1 \times K_d$) and 200 nM concentrations. In the case of
205 rapamycin the lowest concnetration reported in the literature [42,43] to inhibit T cell proliferation
206 by 50% ($1 \times IC_{50} = 20$ pM) was used as the lower dose and 200 pM ($10 \times IC_{50}$) was used as the
207 higher dose.

208 **2.5 Flow cytometry experiments**

209 The flow cytometry measurements were performed on a BD FACScanTM and Facs
210 ArrayTM flow cytometers. We measured the light scatters, namely the forward scatter (FSC) and
211 side scatter (SSC) and the fluorescence intensity on green and red channels. Gate setting for
212 lymphocytes is shown in Fig. 1A, and the gating of viable cells is represented on Fig. 2A and B.
213 The sheath fluid consisted of 1x PBS. Lymphocytes were selected from mixed cell populations
214 of PBMC by their light scatter profile on FACS analysis. Cell proliferation was measured based

215 on the declining CFSE intensity in the green channel (Fig. 1B.). Division index (DI) was used
216 was the the indicator of proliferation and was calculated by this formula

$$217 \quad D = \left(\sum_{k=1}^n A_k \right) / \left(\sum_{k=1}^n A_k \right)$$

218 where k is the division cycle number (i.e. generation number) of cells, and A_k is the cell
219 number in the k^{th} division cycle according to Fig. 1B.

220 **2.6 Measurement of cytokine concentration**

221 Culture supernatants of human peripheral blood mononuclear cells (n=3) were harvested five
222 days after application of mitogens and ion channel blockers, and the concentration of IL-10 and
223 IFN- was measured using OptEIA kits (BD Biosciences, Franklin Lakes, NJ, USA), according
224 to manufacturer's instructions, using duplicates.

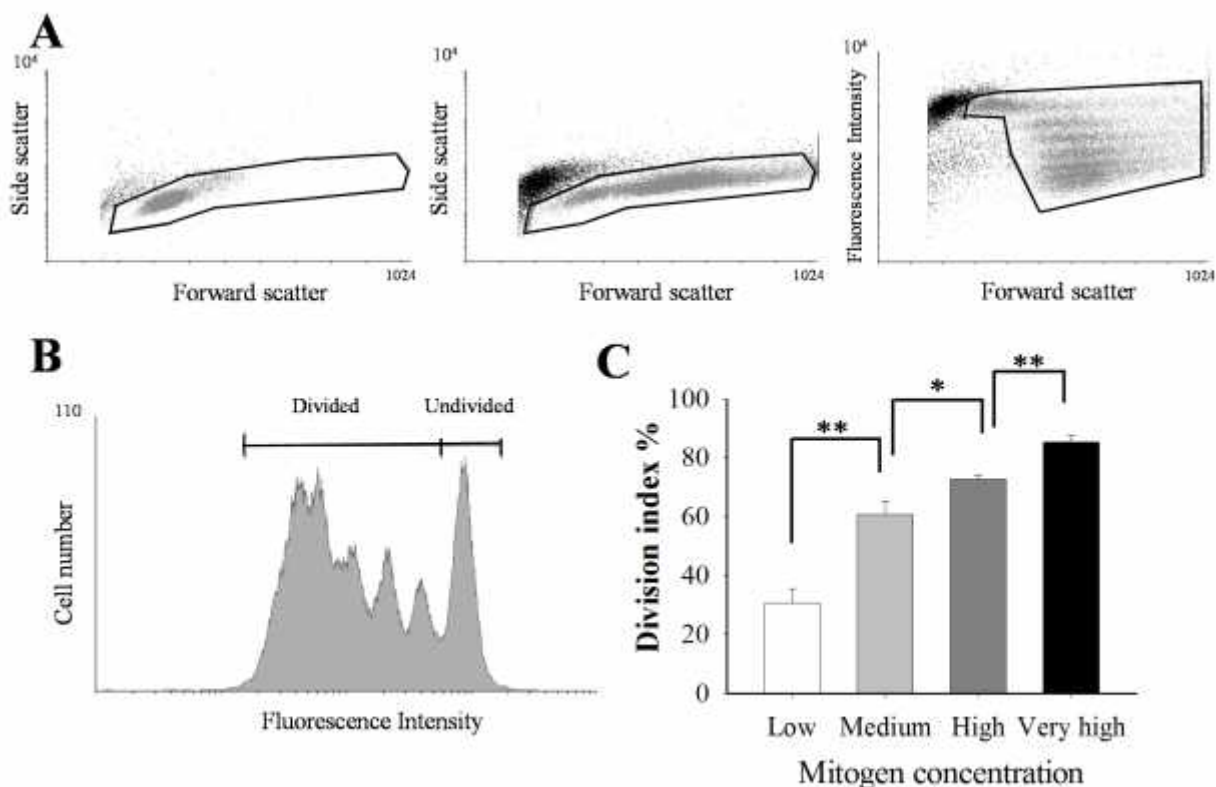
225 **2.7 Data evaluation and statistics**

226 Flow cytometric data were collected using BD CellQuest™ 12.1. For data analysis we
227 used the freeware program Cyflogic 1.2.1. The analyzed data was exported to Microsoft Office
228 Excel™ 2007. For statistical evaluation of our results we used the program SigmaPlot™ 12.0,
229 where we applied one-way ANOVA test and as post hoc analysis, Holm-Sidak test versus the
230 positive control cell population. We marked the level of significance with * if p was <0.05, with
231 **, if p was <0.01, and with ***, if p was <0.001. Data are represented as mean ±S.E.M.

232

234 **3.1 Dose-dependence of mitogen-induced proliferation**

235 As stated in the introduction, our first step was to achieve multiple levels of selective T
 236 lymphocyte stimulation using anti-CD3 and anti-CD28 monoclonal antibodies. Fig. 1. shows that
 237 comparing the division indices (DI) of stimulated PBMC populations 5 days following mitogen
 238 stimulus, four levels of the mitogen effect could be distinguished: low concentration (200 ng/ml
 239 or 1 bead:200 cells) of the mitogen led to a relatively low amount of proliferation, while the
 240 medium (500 ng/ml or 1 bead:50 cells), high (1 μ g/ml or 1 bead:10 cells) and very high
 241 concentrations (3 μ g/ml or 1 bead:1 cells) resulted, as expected, in markedly higher rates of cell
 242 division. The mean DI are $30.6 \pm 4.8\%$, $60.8 \pm 4.5\%$, $72.7 \pm 1.5\%$ and $85.3 \pm 2.4\%$, respectively.
 243 Pairwise comparison of the observed proliferation rates indicated a significant increase with each
 244 subsequent increase in mitogen concentration ($p=0.0036$; $p=0.044$; $p=0.0042$, respectively).



245 **Figure 1. Cell proliferation at different mitogen concentrations.** A) The left and middle dot
246 plots show stimulated PBMC populations stimulated by 1 $\mu\text{g/ml}$ anti-CD3 and anti-CD28
247 monoclonal antibodies on day 0 and day 5, respectively. Solid black line polygons indicate the
248 position of the gates. Activated T cells on day 5 (middle) having higher light scatter properties
249 and mainly dead cells outside the gate are clearly distinguishable. The dot plot on the right shows
250 the FSC/ Fluorescence intensity of the same population as on the middle dot plot, where the
251 gradual decline in the CFSE intensity as a consequence of cell division can be observed. B) The
252 fluorescence intensity histogram shows CFSE fluorescence intensity obtained from the gated
253 population of the dot plot on the right in panel A. The marker above the histogram indicates the
254 divided and the undivided cell populations, and the ratio of divided cells to all gated cells was
255 calculated yielding the division index (DI, see Materials and Methods). C) DI of the cells
256 stimulated by anti-CD3 and anti-CD28 at various mitogen concentrations (low: 200 ng/ml or 1
257 bead:200 cells; medium: 500 ng/ml or 1 bead:50 cells; high: 1 $\mu\text{g/ml}$ or 1 bead:10 cells; and very
258 high concentration: 3 $\mu\text{g/ml}$ or 1 bead:1 cells). The DIs of these populations are shown in Fig 2
259 as positive controls (Pos.) and the DI of inhibitor treatments were normalized to this data.

260 **3.2 Ion channel blockers and rapamycin alone and in combination inhibit lymphocyte** 261 **proliferation**

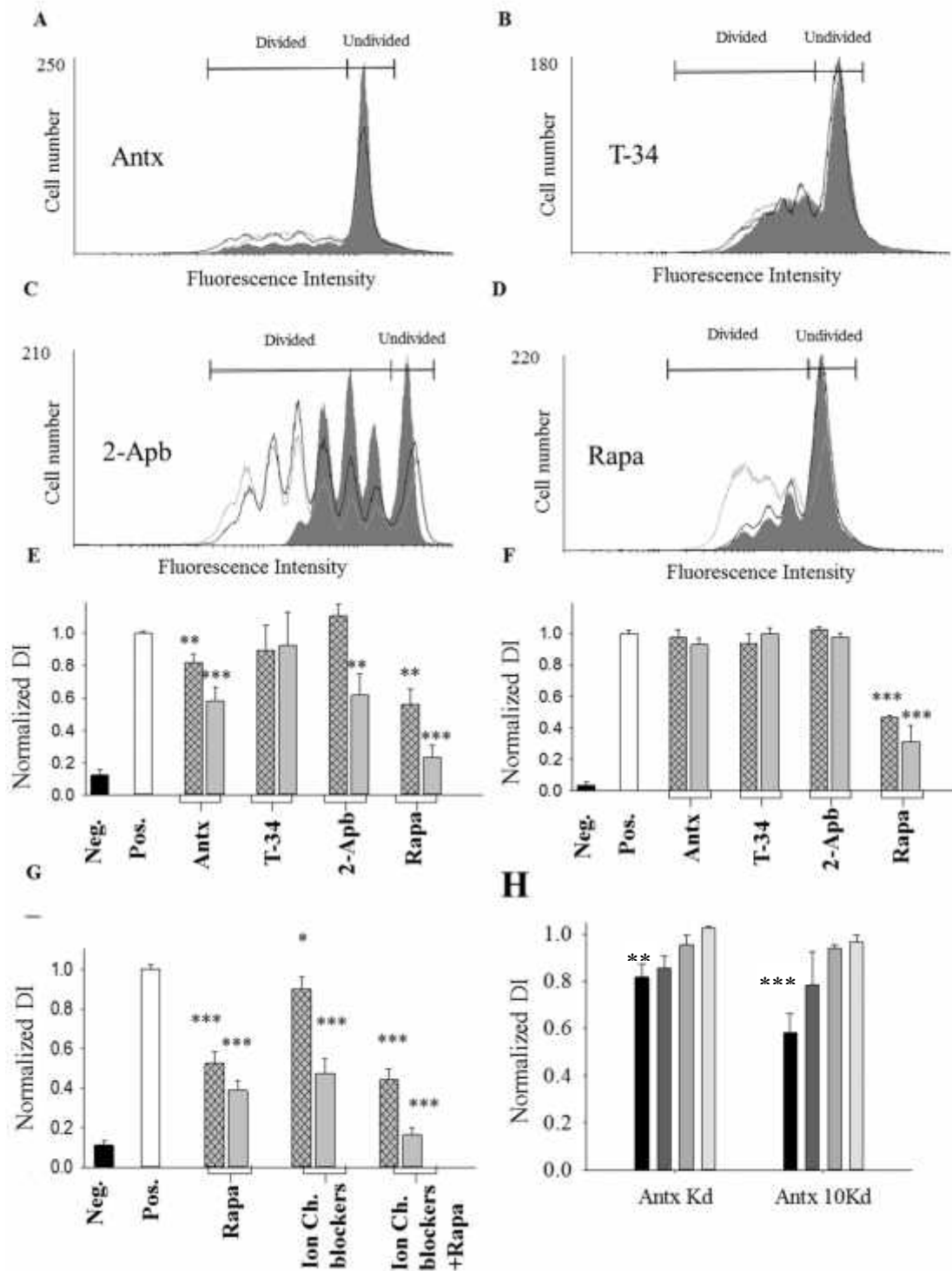
262 The effect of ion channel inhibitors on cell proliferation was tested at a concentration
263 corresponding to the dissociation constant of the drug on the relevant channel ($1 \times K_d$) and at ten
264 times higher concentration ($10 \times K_d$). Rapamycin was used at the lowest IC_{50} obtained from the
265 relevant literature [42,43], and at ten times higher concentration. Figs. 2A-2D show
266 representative fluorescence histograms of the CFSE dilution assay recorded in the absence or in
267 the presence of the blockers in two concentrations. The markedly reduced peaks of the gray-
268 shaded histogram relative to the control light-gray line in Fig. 2A qualitatively show that the
269 Kv1.3 K^+ channel blocker anuroctoxin (Antx) at $10 \times K_d$ concentration inhibited proliferation

270 when the cells were stimulated at low mitogen concentration. Quantitative analysis using
271 normalized DIs (Figs 2E and F) showed that Antx at $1\times K_d$ and $10\times K_d$ concentration inhibited
272 proliferation at low ($p=0.004$, $p<0.001$, respectively), but not at very high ($p=0.930$) mitogen
273 concentration. The nearly superimposable fluorescence histograms in Fig. 2B show that the
274 KCa3.1 inhibitor TRAM-34, regardless of its concentration, caused only a minor reduction of
275 the proliferation of T cells stimulated by low mitogen concentration. The statistical analysis of
276 the DIs (Figs 2E and F) showed that TRAM-34 failed to inhibit cell proliferation both at $1\times K_d$
277 and at $10\times K_d$ concentrations regardless of the mitogen concentration used (at $10\times K_d$ TRAM-34
278 concentration $p=0.489$ and $p=0.993$ for low and very high mitogen concentrations, respectively).
279 The gray-shaded histogram in Fig. 2C shows qualitatively that at low mitogen stimulation the
280 CRAC channel modulator, 2-Aminoethoxydiphenyl borate (2-Apb) applied at $10\times K_d$ blocker
281 concentration inhibited cell proliferation whereas $1\times K_d$ blocker concentration was ineffective.
282 This was confirmed by statistical analysis in Fig. 2E ($p=0.694$ for $1\times K_d$ and $p<0.001$ for $10\times K_d$).
283 Fig. 2F shows that at very high mitogen concentration 2-Apb did not inhibit T cell proliferation
284 even at $10\times K_d$ concentration.

285 The representative histograms in Fig. 2D shows that the mTOR inhibitor rapamycin,
286 applied at both $1\times IC_{50}$ and $10\times IC_{50}$ concentrations markedly inhibits the proliferation of T cells
287 stimulated with low mitogen concentration. This effect was confirmed by the statistical analysis
288 shown in Fig 2E ($1\times IC_{50}$: $p=0.003$; $10\times IC_{50}$: $p<0.001$). As opposed to the ion channel blockers
289 Antx and 2-Apb, rapamycin alone inhibited proliferation even at very high mitogen concentration
290 ($p<0.001$) both at $1\times IC_{50}$ and $10\times IC_{50}$ doses. As shown in Figure 2G, using the combination of
291 all ion channel blockers at $10\times K_d$ concentration led to a marked inhibition of cell proliferation
292 ($p<0.001$), which did not differ from the blocking potential of $10\times IC_{50}$ rapamycin ($p=0.113$).
293 The inhibitory effect of ion channel blockers combined with rapamycin proved to be the most
294 effective treatment, resulting in the complete blockage of cell division ($p<0.001$ compared to

295 control, mean DI=0.163). In the latter case proliferation was not significantly different from the
296 negative control group (mean DI=0.110), which was not stimulated by mitogens (p=0.515).

297 Data above showed that the Kv1.3 blocker Antx and the CRAC channel blocker 2-Apb
298 interfered with T cell proliferation only if cells were stimulated at low mitogen concentration but
299 were ineffective if cells were stimulated with very high mitogen concentration. To further explore
300 this phenomenon, we measured the normalized DI at varying mitogen concentrations (low,
301 medium, high and very high, see above) in the presence of $1\times K_d$ (Fig. 2H left panel) or $10\times K_d$
302 (Fig. 2H right panel) concentrations of Antx. As shown in Fig. 2H right panel a marked inhibition
303 of cell division was observed when the combination of low mitogen and $10\times K_d$ blocker
304 concentration (black bar) was used (p<0.001). At medium, high and very high mitogen
305 concentrations the inhibition of proliferation was not statistically significant as compared to the
306 positive control (p=0.089, 0.372 and 0.742, respectively), but a clear decreasing trend is seen in
307 the effectiveness of the blockers with increasing mitogen concentration. The same tendency
308 could be observed if Antx was applied at $1\times K_d$ concentration (Fig. 2H left panel). The inhibition
309 of proliferation was statistically significant only if low mitogen concentration (p=0.004) was
310 used whereas at medium, high, and very high mitogen concentrations the inhibition of
311 proliferation did not prove to be significant (p=0.365, 0.955 and 0.964 at medium, high and very
312 high mitogen concentrations, respectively).



313

314

315 **Figure 2. Effect of ion channel blockers and rapamycin on cell proliferation.** A-D) The
 316 representative fluorescence histograms corresponding to the CFSE dilution assay (see methods)
 317 show the effect of four inhibitors on T cell proliferation. Light gray lines in the histograms

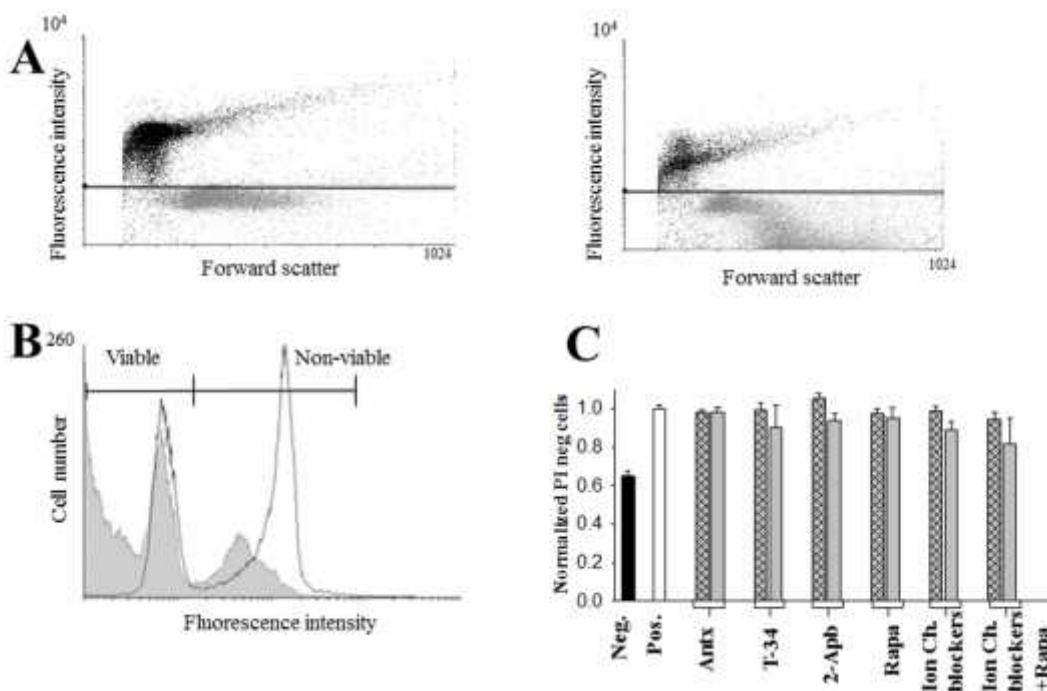
318 indicate the positive control population (Pos.) treated solely with mitogens, black lines and gray
319 filled histograms indicate data obtained in the presence of a blocker at $1 \times K_d$ and $10 \times K_d$
320 concentrations, respectively (A: Antx, 500pM ($1 \times K_d$) and 5 nM; B: TRAM-34 (T-34), 20 nM
321 ($1 \times K_d$) and 200 nM; C: 2-Apb, 5 μ M ($1 \times K_d$) and 50 μ M; D: rapamycin (Rapa), 20 pM ($1 \times IC_{50}$)
322 and 200 pM ($10 \times IC_{50}$)). Cells were stimulated with low mitogen concentration in each case (200
323 ng/ml anti-CD3 and 1 μ g/ml anti-CD28 or 1 bead:200 cells). E-F) Proliferation, represented by
324 DI (see Figure 1.), at low (Fig. 2E, 200 ng/ml anti-CD3 and 1 μ g/ml anti-CD28 or 1 bead:200
325 cells) or very high (Fig. 2F, 3 μ g/ml and 1 μ g/ml anti-CD28 or 1 bead:1 cell) mitogen
326 concentrations in the presence of $1 \times K_d$ (cross-hatched bars) and $10 \times K_d$ (gray) blocker
327 concentrations (for concentrations, see above). Neg. indicates the negative control population,
328 where cells were not stimulated by mitogens, but were stained with CFSE. The DIs of samples
329 treated with different blockers were normalized to the average DI of the Pos. sample. G)
330 Comparison of the effectiveness of treatment combinations as compared to the positive control
331 (Pos.). During the combined treatments each blocker was applied at its $1 \times K_d$ (cross-hatched) or
332 $10 \times K_d$ (gray) concentration, data obtained for different mitogen concentrations were pooled for
333 the analysis. H) Mitogen-dependence of the inhibition of cell proliferation. The DIs were
334 determined in the presence of Antx at $1 \times K_d$ (left) or $10 \times K_d$ (right), at low (black), medium (dark
335 gray), high (gray) and very high (light gray) mitogen concentrations (see legend to Fig. 1). Error
336 bars indicate SEM, asterisks indicate significance (* if p was <0.05 , with **, if p was <0.01 , and
337 with ***, if p was <0.001)

338

339 **3.3 Cell viability is not affected by inhibitors of T cell proliferation**

340 The reduced proliferation in the presence of the ion channel blockers and rapamycin (see
341 above, Fig. 2) might be induced by a decrease in the viability of the cells in the presence of these

342 compounds. This was tested in the experiments shown in Fig. 3 using a propidium iodide uptake
 343 assay. The dot-plots in Fig. 3A show the threshold discriminating viable and non-viable cells
 344 using the combination of forward scatter and PI fluorescence. The corresponding fluorescence
 345 histograms in Fig 3B show that stimulation of the cells increased the proportion of the viable
 346 cells. The proportion of viable cells was not altered either by the ion channel blockers or
 347 rapamycin alone, or in their various combinations regardless of the concentration of the
 348 compounds (Fig. 3C, $1\times K_d$: $p=0.903, 0.902, 0.652$ and 0.508 for Antx, TRAM-34, 2-Apb and
 349 rapamycin, respectively; or $10\times K_d$: $p=0.871, 0.867, 0.740$ and 0.225 for Antx, TRAM-34, 2-Apb
 350 and rapamycin, respectively; $p=0.244$ for their combination).



351
 352 **Figure 3. Effect of ion channel blockers and rapamycin on the cellular viability.** A) The dot
 353 plots show the standard gating strategy for propidium iodide (PI) staining. The left panel indicates
 354 non-stimulated (Neg.), the right panel shows the stimulated population (Pos.) after 5 days of
 355 incubation with superparamagnetic bead-conjugated anti-CD3 and anti-CD28 monoclonal
 356 antibodies at 1 bead:1 cells ratio. The horizontal black line indicates the threshold for

357 discriminating live and non-live cells. B) The fluorescence histograms were generated from the
358 dot plots shown in A, the bar and the markers indicate the PI negative viable and the PI positive
359 non-viable cells in the Neg. (black line) and Pos. (gray fill) samples. C) Viability of the cell
360 populations in the presence of inhibitors. The number of PI negative cells in the presence of
361 various compounds was normalized to that of the untreated, but activated cells (Pos. sample).
362 Cross-hatched and gray bars show data obtained in the presence of $1\times K_d$ and $10\times K_d$
363 concentrations of the indicated compounds alone or in mixtures (T-34: TRAM-34, Rapa:
364 rapamycin). Mixtures of ion channel blockers contained each blocker at $1\times K_d$ or $10\times K_d$ (Ion Ch.
365 blockers) whereas in the Ion Ch. Blockers+Rapa samples the ion channel blocker mixture is
366 supplemented with the corresponding concentrations of rapamycin ($1\times IC_{50}$ or $10\times IC_{50}$). Error
367 bars indicate SEM.

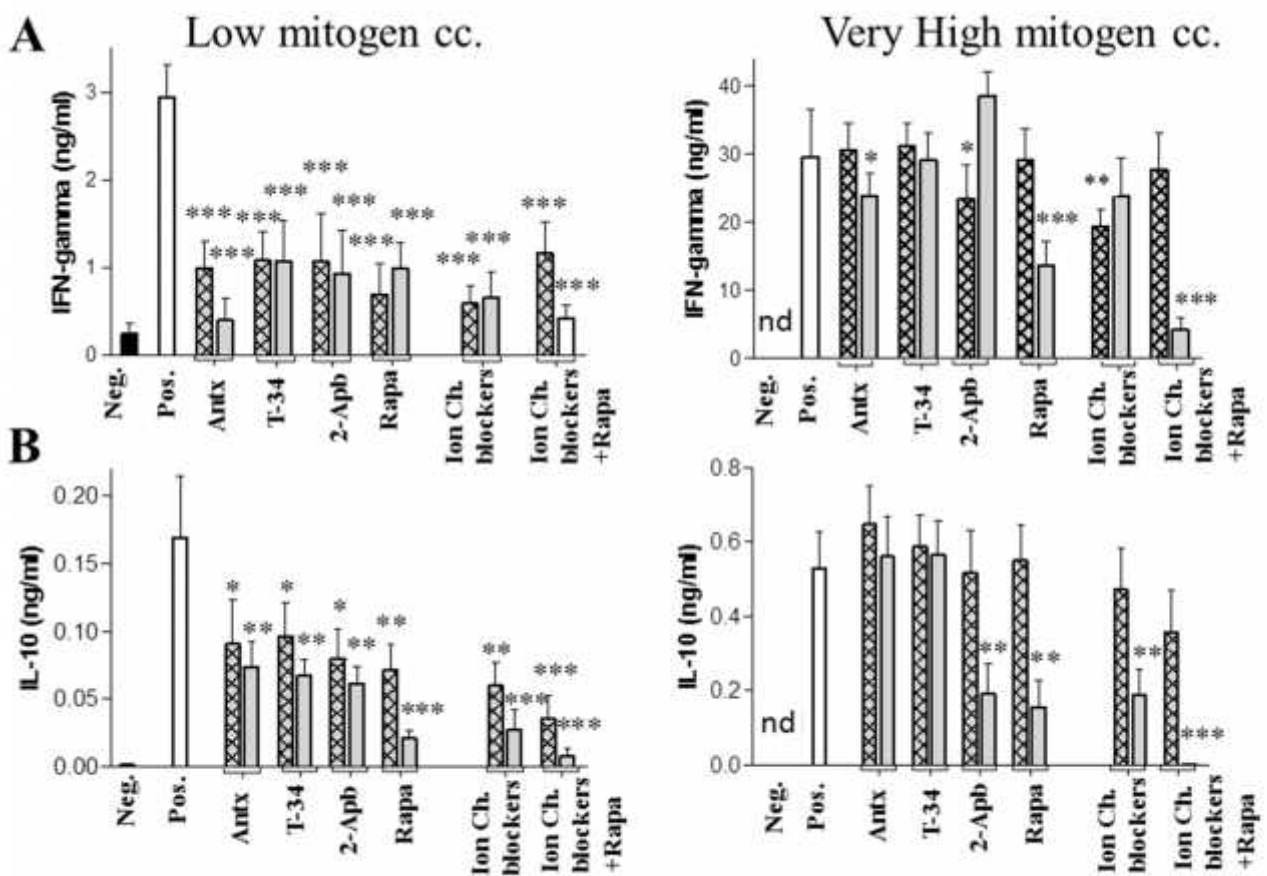
368

369 **3.4 Cytokine production of T cells can be reduced by ion channel blockers**

370 We investigated the effect of channel blockers and rapamycin on the secretion of the anti-
371 inflammatory IL-10 and the pro-inflammatory IFN- γ cytokines by ELISA. Increasing the
372 mitogen concentration from low to very high induced approximately 4-fold and 10-fold increases
373 in secreted IL-10 and IFN- γ levels, respectively (Fig. 4. A and B, Pos.). IFN- γ as well as IL-10
374 secretion was significantly inhibited at low mitogen stimulation by all inhibitors and
375 combinations at both applied concentrations (Fig. 4. A and B, left panels) (IFN- γ : $p<0.001$ for
376 all inhibitors; IL-10: Antx $1\times K_d$ $p=0.046$, $10\times K_d$ $p=0.024$, TRAM-34 $1\times K_d$ $p=0.048$, $10\times K_d$
377 $p=0.008$, 2-Apb $1\times K_d$ $p=0.039$, $10\times K_d$ $p=0.007$, rapamycin $1\times K_d$ $p=0.009$, $10\times K_d$ $p<0.001$, ion
378 channel blockers $1\times K_d$ $p=0.002$, $10\times K_d$ $p<0.001$, ion channel blockers together with rapamycin
379 $1\times K_d$ and $10\times K_d$ $p<0.001$). At very high mitogenic stimulation IFN- γ secretion was inhibited by
380 Antx, rapamycin and combination treatments at $10\times K_d$ and by 2-Apb and the ion channel

381 blocker combination at $1 \times K_d$ (Fig. 4A right panel) (Antx $10 \times K_d$ $p=0.041$, 2-Apb $1 \times K_d$ $p=0.049$,
 382 rapamycin $10 \times K_d$ $p<0.001$, ion channel blockers $1 \times K_d$ $p=0.002$, ion channel blockers together
 383 with rapamycin $p<0.001$). IL-10 production was only inhibited by $10 \times K_d$ 2-Apb, rapamycin and
 384 combination treatments (Fig 4B right panel) (2-Apb $10 \times K_d$: 0.004, rapamycin $10 \times K_d$: 0.002 , ion
 385 channel blockers $p=0.004$, ion channel blockers together with rapamycin: $p<0.001$).

386



387 **Figure 4. Inhibition of cytokine secretion by ion channel blockers and rapamycin**

388 A) IFN- and B) IL-10 secretion were measured using ELISA (OptEIA kit) at different mitogen
 389 concentrations, respectively. Left and right panels refer to data obtained at low and very high
 390 mitogen concentrations. Neg. indicates the unstimulated control cell population whereas Pos.
 391 indicates the mitogen-stimulated cell population in the absence of ion channel blockers and/or

392 rapamycin. The blockers are represented at $1 \times K_d$ (cross-hatched), $10 \times K_d$ (gray) or in case of
393 rapamycin $1 \times IC_{50}$ and $10 \times IC_{50}$ concentrations, respectively. Error bars indicate SEM, asterisks
394 indicate significance (* if p was <0.05 , with **, if p was <0.01 , and with ***, if p was <0.001),
395 and n.d. indicates “not detectable” where values are too low to be shown.

396

397

Discussion

398 Altered T cell homeostasis is involved in the pathogenesis of autoimmune diseases such
399 as multiple sclerosis [44] and systemic lupus erythematosus [45]. To maximize anti-proliferative
400 effects and to reduce potential side effects, immunosuppressive drugs are commonly used in
401 combinations [46]. One group of the most promising candidates for future therapy is the family
402 of Kv1.3 inhibitors, because this ion channel is found only in a few tissues and it can be inhibited
403 selectively [28]. Before applying ion channel blockers in therapy it is crucial to investigate how
404 they interact with other immunosuppressive agents. However, original research data about the
405 pharmacodynamics of combinations of traditional immunosuppressive and novel drugs such as
406 ion channel blockers are scarce and they usually lack functional comparison. Therefore, in our
407 recent experiments, we approached this problem from multiple aspects and have found an
408 additive interaction between rapamycin and the ion channel blockers when using them in
409 combination.

410 The effects of ion channel blockers exerted on T cell functions have already been
411 described [17]. However, to the best of our knowledge, no data comparing the proliferative
412 effects of Kv1.3, KCa3.1 and CRAC channel blockers applied alone or in combination at
413 identical experimental conditions are currently available. Moreover, the synergy between the
414 effects of ion channel inhibitors and the mTOR inhibitor rapamycin has not been investigated to
415 date. In the present study we are the first to describe the mitosis-inhibiting effect of Antx, a high
416 affinity scorpion toxin blocker of Kv1.3 [40] both at high ($10\times K_d$) and low ($1\times K_d$) concentrations.
417 The observed effect of 2-Apb correlated well with past literature, as it was proposed that 2-Apb
418 has a bimodal effect. At low blocker concentrations (K_d), 2-Apb promotes Ca^{2+} signaling, which
419 ultimately results in enhanced cell proliferation, whereas at higher concentrations, in our case at
420 $10\times K_d$, it effectively inhibits the CRAC channel, ultimately blocking cellular proliferation [47].

421 Even low mitogen concentrations, which corresponded to 1:200 bead:cell ratio produced
422 an unexpectedly high amount of polyclonal lymphocyte proliferation, as over 30% of the cells
423 have undergone cell division. This phenomenon may be explained by the fact that there is a large
424 number of anti-CD3 and anti-CD28 molecules on a single bead, and that lymphocytes form a
425 rosette-like structure around beads. Therefore, numerous lymphocytes are activated
426 simultaneously by a single bead, and this effect could be further enhanced by autocrine and
427 paracrine cytokine secretion of the activated T cells [48,49].

428 Our most intriguing finding in this research was that increasing the mitogen concentration
429 markedly decreased the anti-proliferative effect of ion channel blockers that ultimately
430 completely disappeared when cells were stimulated with very high concentration of the mitogens.
431 A possible explanation may be that at low mitogen concentrations the few, initially highly
432 localized Ca^{2+} signals are suppressed by the blocked ion channels in their immediate vicinity
433 [50]. However, at very high mitogen concentration when most TCRs are likely to be activated,
434 the number of localized signaling loci is sufficiently high so that even a very low fraction of
435 unblocked ion channels is sufficient to maintain the downstream activation cascade upon TCR
436 activation. Moreover, it is reasonable to assume that lymphocytes redirect their activation
437 pathways to other, Ca^{2+} -independent directions. As several intracellular signaling pathways, e.g.
438 mTOR activation, do not essentially involve ion channels [29,30], these processes may become
439 overly active upon applying very high mitogen concentrations. However, to the best of our
440 knowledge no study has ever addressed this question and thus it warrants further experiments.

441 At very high mitogen concentrations we could achieve significant blockage of
442 proliferation only by using rapamycin or its combination with the ion channel blockers acting on
443 a different pathway that ultimately leads to permanent changes in cellular signaling. This may
444 indicate that co-treatment of T cells with rapamycin and ion channel blockers may be a more
445 feasible therapeutical approach than using these drugs separately.

446 Previous studies have shown that blocking Kv1.3 channels without affecting the KCa3.1
447 channels inhibited IFN- γ expression in a subset of T-cells with effector memory phenotype (T_{EM})
448 [51]. Moreover, the blockage of CRAC channels with SKF 96365 decreased both IL-10 and IFN- γ
449 production [52]. In line with these studies our data showed that treatment of T-cells with various
450 inhibitors (Fig. 4) significantly decreased both anti-inflammatory IL-10 and inflammatory IFN- γ
451 cytokine production but only at low mitogenic stimulation. In accordance with the literature
452 TRAM-34 strongly suppressed cytokine production despite the fact that it did not inhibit
453 proliferation [14,34]. At very high mitogen concentration the effect of the ion channel blockers
454 on cytokine production diminished. Although some of them caused statistically significant
455 reductions in cytokine production, these changes are not likely to be biologically relevant as the
456 remaining concentration of IFN- γ still remained in the ng/ml range and therefore was sufficient
457 to promote cell proliferation, so division rate was unaffected. In contrast, rapamycin and the
458 combination treatments applied at $10 \times K_d$ concentration caused a more robust decrease, which
459 was also reflected in the suppressed proliferation of these cells.

460 Since IL-10 and IFN- γ levels were affected in a qualitatively similar manner by the
461 inhibitors both at low and very high mitogen concentrations, it is safe to assume that these
462 treatments did not alter the proportion of T cell subtypes specifically (i.e. Th₁ CD4 and CD8
463 cytotoxic T cells vs. Th₂ T cells and regulatory CD4⁺/CD25⁺/FoxP3⁺ T_{reg} cells), but rather were
464 affecting globally the entire T cell population.

465 In summary, the greatest level of inhibition of T-cell proliferation and the production of
466 selected cytokines could be achieved by rapamycin, and this effect could be further potentiated
467 by using it in combination with cation channel blockers. This may indicate an additive effect of
468 Ca²⁺-dependent and Ca²⁺-independent inhibitory mechanisms involved in T-cell activation.
469 Finally, we found that upon increasing the concentration of the mitogenic antibodies, the anti-
470 proliferative effect of ion channel blockers faded. This phenomenon can be due to a yet unknown

471 mechanism in intracellular signaling of activated T cells, which is to be elucidated in the future.
472 The increased *in vitro* antiproliferative potency of rapamycin and ion channel blocker
473 combination presented in this study urges for *in vivo* experiments whereby the therapeutic benefit
474 of the combined treatment can be assessed.

475

476

4. Acknowledgments

477 The study was supported by KTIA_NAP_13-2-2015-0009 (Z.V.) and Z.V. is Bolyai
478 Fellowship awardee. We thank Cecilia Nagy for excellent technical assistance. Moreover, we are
479 grateful for the help of the healthy volunteers. Finally, we greatly appreciate helpful discussions
480 with the co-workers of the Institute of Biophysics and Cell Biology.

481

5. Conflict of interest

482 The authors declare no commercial and financial conflict of interest regarding this project.

483

484

485

6. *Vitae*

486 Zoltan Petho, graduate student at the University of Debrecen, MD:

487 He studies the ion channels of the immune system and of cancer cells. During
488 his medical studies his main interest were the voltage-gated ion channels of T-
489 cells and their potential functional implications. Currently he is also focused on
490 the ion channels of invasive cells and their roles in tumor metastasis. He is
491 skilled in proliferation assays, flow cytometry, functional studies such as
492 migration and invasion assays and patch-clamp electrophysiology.



493

494 Andras Balajthy, graduate student at the University of Debrecen, MD:

495 His main interest is to study the interaction of cholesterol and voltage gated ion
496 channels. Currently he studies the Kv1.3 ion channels of lymphocytes isolated
497 from Smith-Lemli-Opitz syndrome. He is a well-trained electrophysiologist,
498 but also familiar with flow-cytometry and confocal microscopy.



499

500 Adam Bartok: postdoctoral fellow at the Thomas Jefferson University, Philadelphia, PhD:

501 He is experienced in K⁺ channel electrophysiology. During his graduate
502 research in Gyorgy Panyi's lab, he focused mainly on the pharmacology of
503 peptide toxins using patch-clamp technique. Moreover, he is skilled in
504 measurements of mitochondrial calcium signaling, recombinant protein
505 synthesis, fluorescence measurements, confocal microscopy and electron
506 microscopy.



507

508 Krisztian Bene, predoctor at the University of Debrecen:

509 He is predictor at the research group headed by Éva Rajnavölgyi in the
510 University of Debrcen and focuses on the biology of human dendritic cells
511 (DC). He studies the effects of microbial antigens on inflammation and T
512 lymphocyte activation mediated by different DC populations. He plays also
513 part in analyzing the role of cell signaling pathways related to pro-
514 inflammatory cytokine and type I. interferon production in DC.



515

516 Sandor Somodi, assistant professor at University of Debrecen, MD, PhD

517 Sandor Somodi completed his PhD in 2007 at the University of Debrecen.

518 During his graduate research he studied inactivation kinetics and
519 pharmacology of the Kv1.3 channel. Recently, he works at the Internal
520 Medicine Department focusing on metabolic diseases and mainly lipid
521 disorders. He is skilled in ion channel pharmacology and patch clamp electrophysiology.



522

523 Orsolya Szilagyi, postdoctoral fellow at the National Institute of Health, PhD

524 Orsolya Szilagyi completed her PhD in 2014 in molecular medicine at the

525 University of Debrecen in 2014. During her PhD she spent three months at the

526 University of Cincinnati as a visiting scientist. Currently, her scientific interests

527 include elucidating the function of various voltage sensor proteins both in the

528 immune and the nervous system by the means of biophysical methods such as

529 electrophysiology (patch clamp, voltage clamp fluorometry) and confocal microscopy.



530

531

532

533 Eva Rajnavolgyi, Professor of Immunology at the University of Debrecen, PhD, DSc:

534 She has a long lasting experience in studying the interplay of innate and adaptive

535 immune responses with a focus to DC subtypes/subsets driving anti-microbial

536 defense. Currently, she is interested in identifying cellular mechanisms regulating

537 the collaboration of signaling pathways driving anti-viral immune responses. She

538 is also involved in uncovering the impact of retinoic acid induced gene-I (RIG-I)

539 and mesenchymal stromal cells (MSC) on the outcome of DC-induced immune

540 responses. Recently, her research group described the role of mTOR in the regulation of

541 monocyte-derived and CD1c+ DC functions.

542

543 Zoltan Varga, Senior research fellow, Head of the MTA-DE-NAP B Ion Channel Structure-

544 Function Research Group, RCMM, University of Debrecen, PhD, DSc:

545 He is experienced in studying the gating of voltage-gated ion channels including

546 voltage-sensor movements. Moreover he uncovered many aspects of the

547 pharmacology of voltage-gated K⁺ channels, especially Kv channel and characterized

548 multiple blocking scorpion toxins. Moreover he is also involved in C-type inactivation

549 of ion channels and the effect of ionic conditions and pH on channel gating.

550

551 Gyorgy Panyi Professor of Biophysics at the University of Debrecen, M.D., Ph.D., D.Sc.:

552 Gyorgy Panyi is engaged in unveiling the functional and biophysical characteristics

553 of voltage-gated ion channels. His research projects focus on two types of ion

554 channels of T-lymphocytes, the voltage-gated K⁺ channel, Kv1.3, and the Ca²⁺-

555 activated K⁺ channel, KCa3.1. Understanding the biophysical properties of Kv1.3

556 and KCa3.1 and their regulation may be critical to our comprehension of T-cell

557 physiology and immune responsiveness.



- 561 [1] Mazza C, Malissen B. What guides MHC-restricted TCR recognition? *Seminars in immunology* 2007;19:225-235.
- 562
- 563 [2] Samelson LE. Signal transduction mediated by the T cell antigen receptor: the role of adapter proteins. *Annual review of immunology* 2002;20:371-394.
- 564
- 565 [3] Larbi A, Pawelec G, Wong SC, Goldeck D, Tai JJ, Fulop T. Impact of age on T cell signaling: a general defect or specific alterations? *Ageing research reviews* 2011;10:370-378.
- 566
- 567 [4] Purtic B, Pitcher LA, van Oers NS, Wulfing C. T cell receptor (TCR) clustering in the immunological synapse integrates TCR and costimulatory signaling in selected T cells. *Proceedings of the National Academy of Sciences of the United States of America* 2005;102:2904-2909.
- 568
- 569
- 570
- 571 [5] Szilagyi O, Boratko A, Panyi G, Hajdu P. The role of PSD-95 in the rearrangement of Kv1.3 channels to the immunological synapse. *Pflugers Archiv : European journal of physiology* 2013;465:1341-1353.
- 572
- 573
- 574 [6] Lenschow DJ, Walunas TL, Bluestone JA. CD28/B7 system of T cell costimulation. *Annual review of immunology* 1996;14:233-258.
- 575
- 576 [7] Jiang H, Chess L. Regulation of immune responses by T cells. *The New England journal of medicine* 2006;354:1166-1176.
- 577
- 578 [8] Rochman Y, Spolski R, Leonard WJ. New insights into the regulation of T cells by gamma(c) family cytokines. *Nature reviews Immunology* 2009;9:480-490.
- 579
- 580 [9] Li Y, Kurlander RJ. Comparison of anti-CD3 and anti-CD28-coated beads with soluble anti-CD3 for expanding human T cells: differing impact on CD8 T cell phenotype and responsiveness to restimulation. *Journal of translational medicine* 2010;8:104.
- 581
- 582
- 583 [10] Trickett A, Kwan YL. T cell stimulation and expansion using anti-CD3/CD28 beads. *Journal of immunological methods* 2003;275:251-255.
- 584
- 585 [11] Ceuppens JL, Baroja ML, Lorre K, Van Damme J, Billiau A. Human T cell activation with phytohemagglutinin. The function of IL-6 as an accessory signal. *Journal of immunology* 1988;141:3868-3874.
- 586
- 587
- 588 [12] Lyall RM, Crumpton MJ. Ionomycin Stimulates Lymphocyte Growth and Promotes the Activity of Lymphocyte-T Mitogens. *Immunobiology* 1981;159:168-169.
- 589
- 590 [13] Olsen I, Sollid LM. Pitfalls in determining the cytokine profile of human T cells. *J Immunol Methods*;390:106-112.
- 591
- 592 [14] Schoenborn JR, Wilson CB. Regulation of interferon-gamma during innate and adaptive immune responses. *Adv Immunol* 2007;96:41-101.
- 593
- 594 [15] Matteson DR, Deutsch C. K channels in T lymphocytes: a patch clamp study using monoclonal antibody adhesion. *Nature* 1984;307:468-471.
- 595
- 596 [16] DeCoursey TE, Chandy KG, Gupta S, Cahalan MD. Voltage-gated K⁺ channels in human T lymphocytes: a role in mitogenesis? *Nature* 1984;307:465-468.
- 597
- 598 [17] Cahalan MD, Chandy KG. The functional network of ion channels in T lymphocytes. *Immunological reviews* 2009;231:59-87.
- 599
- 600 [18] Cahalan MD, Wulff H, Chandy KG. Molecular properties and physiological roles of ion channels in the immune system. *Journal of clinical immunology* 2001;21:235-252.
- 601
- 602 [19] Luik RM, Lewis RS. New insights into the molecular mechanisms of store-operated Ca²⁺ signaling in T cells. *Trends in molecular medicine* 2007;13:103-107.
- 603
- 604 [20] Varga Z, Hajdu P, Panyi G. Ion channels in T lymphocytes: an update on facts, mechanisms and therapeutic targeting in autoimmune diseases. *Immunology letters* 2010;130:19-25.
- 605
- 606 [21] Logsdon NJ, Kang J, Togo JA, Christian EP, Aiyar J. A novel gene, hKCa4, encodes the calcium-activated potassium channel in human T lymphocytes. *The Journal of biological chemistry* 1997;272:32723-32726.
- 607
- 608

- 609 [22] Begenisich T, Nakamoto T, Ovitt CE, Nehrke K, Brugnara C, Alper SL, et al. Physiological roles of
610 the intermediate conductance, Ca²⁺-activated potassium channel Kcnn4. *The Journal of*
611 *biological chemistry* 2004;279:47681-47687.
- 612 [23] Melzer N, Hicking G, Gobel K, Wiendl H. TRPM2 cation channels modulate T cell effector
613 functions and contribute to autoimmune CNS inflammation. *PloS one* 2012;7:e47617.
- 614 [24] Lewis RS, Ross PE, Cahalan MD. Chloride channels activated by osmotic stress in T
615 lymphocytes. *The Journal of general physiology* 1993;101:801-826.
- 616 [25] Wulff H, Calabresi PA, Allie R, Yun S, Pennington M, Beeton C, et al. The voltage-gated Kv1.3
617 K(+) channel in effector memory T cells as new target for MS. *The Journal of clinical*
618 *investigation* 2003;111:1703-1713.
- 619 [26] Robert V, Triffaux E, Savignac M, Pelletier L. [Calcium signaling in T lymphocytes]. *Medecine*
620 *sciences : M/S* 2012;28:773-779.
- 621 [27] Wulff H, Beeton C, Chandy KG. Potassium channels as therapeutic targets for autoimmune
622 disorders. *Current opinion in drug discovery & development* 2003;6:640-647.
- 623 [28] Beeton C, Wulff H, Standifer NE, Azam P, Mullen KM, Pennington MW, et al. Kv1.3 channels
624 are a therapeutic target for T cell-mediated autoimmune diseases. *Proceedings of the National*
625 *Academy of Sciences of the United States of America* 2006;103:17414-17419.
- 626 [29] Chen J, Fang Y. A novel pathway regulating the mammalian target of rapamycin (mTOR)
627 signaling. *Biochemical pharmacology* 2002;64:1071-1077.
- 628 [30] Gingras AC, Raught B, Sonenberg N. Regulation of translation initiation by FRAP/mTOR. *Genes*
629 *& development* 2001;15:807-826.
- 630 [31] Saunders RN, Metcalfe MS, Nicholson ML. Rapamycin in transplantation: a review of the
631 evidence. *Kidney international* 2001;59:3-16.
- 632 [32] Witkowski JM, Siebert J, Lukaszuk K, Trawicka L. Comparison of effect of a panel of membrane
633 channel blockers on the proliferative, cytotoxic and cytoadherence abilities of human
634 peripheral blood lymphocytes. *Immunopharmacology* 1993;26:53-63.
- 635 [33] Jensen BS, Odum N, Jorgensen NK, Christophersen P, Olesen SP. Inhibition of T cell
636 proliferation by selective block of Ca(2+)-activated K(+) channels. *Proceedings of the National*
637 *Academy of Sciences of the United States of America* 1999;96:10917-10921.
- 638 [34] Wulff H, Miller MJ, Hansel W, Grissmer S, Cahalan MD, Chandy KG. Design of a potent and
639 selective inhibitor of the intermediate-conductance Ca²⁺-activated K⁺ channel, IKCa1: a
640 potential immunosuppressant. *Proceedings of the National Academy of Sciences of the United*
641 *States of America* 2000;97:8151-8156.
- 642 [35] Schmitz A, Sankaranarayanan A, Azam P, Schmidt-Lassen K, Homerick D, Hansel W, et al.
643 Design of PAP-1, a selective small molecule Kv1.3 blocker, for the suppression of effector
644 memory T cells in autoimmune diseases. *Molecular pharmacology* 2005;68:1254-1270.
- 645 [36] Pegoraro S, Lang M, Dreker T, Kraus J, Hamm S, Meere C, et al. Inhibitors of potassium
646 channels KV1.3 and IK-1 as immunosuppressants. *Bioorganic & medicinal chemistry letters*
647 2009;19:2299-2304.
- 648 [37] Lyons AB, Parish CR. Determination of lymphocyte division by flow cytometry. *Journal of*
649 *immunological methods* 1994;171:131-137.
- 650 [38] Lyons AB. Analysing cell division in vivo and in vitro using flow cytometric measurement of
651 CFSE dye dilution. *Journal of immunological methods* 2000;243:147-154.
- 652 [39] Lyons AB, Blake SJ, Doherty KV. Flow cytometric analysis of cell division by dilution of CFSE and
653 related dyes. *Current protocols in cytometry / editorial board, J Paul Robinson, managing*
654 *editor [et al]* 2013;Chapter 9:Unit9 11.
- 655 [40] Bagdany M, Batista CV, Valdez-Cruz NA, Somodi S, Rodriguez de la Vega RC, Licea AF, et al.
656 Anuroctoxin, a new scorpion toxin of the alpha-KTx 6 subfamily, is highly selective for Kv1.3
657 over IKCa1 ion channels of human T lymphocytes. *Molecular pharmacology* 2005;67:1034-
658 1044.
- 659 [41] Bootman MD, Collins TJ, Mackenzie L, Roderick HL, Berridge MJ, Peppiatt CM. 2-
660 aminoethoxydiphenyl borate (2-APB) is a reliable blocker of store-operated Ca²⁺ entry but an

661 inconsistent inhibitor of InsP3-induced Ca²⁺ release. *FASEB journal : official publication of the*
662 *Federation of American Societies for Experimental Biology* 2002;16:1145-1150.

663 [42] Ghez D, Rubio MT, Maillard N, Suarez F, Chandesris MO, Delarue R, et al. Rapamycin for
664 refractory acute graft-versus-host disease. *Transplantation* 2009;88:1081-1087.

665 [43] Wang X, Omura S, Szweda LI, Yang Y, Berard J, Seminaro J, et al. Rapamycin inhibits
666 proteasome activator expression and proteasome activity. *European journal of immunology*
667 1997;27:2781-2786.

668 [44] Venken K, Hellings N, Liblau R, Stinissen P. Disturbed regulatory T cell homeostasis in multiple
669 sclerosis. *Trends in molecular medicine* 2010;16:58-68.

670 [45] Tsokos GC, Nambiar MP, Tenbrock K, Juang YT. Rewiring the T-cell: signaling defects and novel
671 prospects for the treatment of SLE. *Trends in immunology* 2003;24:259-263.

672 [46] Nevins TE. Overview of new immunosuppressive therapies. *Current opinion in pediatrics*
673 2000;12:146-150.

674 [47] Goto J, Suzuki AZ, Ozaki S, Matsumoto N, Nakamura T, Ebisui E, et al. Two novel 2-aminoethyl
675 diphenylborinate (2-APB) analogues differentially activate and inhibit store-operated Ca(2+)
676 entry via STIM proteins. *Cell calcium* 2010;47:1-10.

677 [48] Kim DT, Rothbard JB, Bloom DD, Fathman CG. Quantitative analysis of T cell activation: role of
678 TCR/ligand density and TCR affinity. *Journal of immunology* 1996;156:2737-2742.

679 [49] Arakaki A, Ooya K, Akiyama Y, Hosokawa M, Komiyama M, Iizuka A, et al. TCR-beta repertoire
680 analysis of antigen-specific single T cells using a high-density microcavity array. *Biotechnology*
681 *and bioengineering* 2010;106:311-318.

682 [50] Parekh AB. Ca²⁺ microdomains near plasma membrane Ca²⁺ channels: impact on cell
683 function. *J Physiol* 2008;586:3043-3054.

684 [51] Xu R, Cao M, Wu X, Wang X, Ruan L, Quan X, et al. Kv1.3 channels as a potential target for
685 immunomodulation of CD4⁺ CD28null T cells in patients with acute coronary syndrome. *Clin*
686 *Immunol* 2012;142:209-217.

687 [52] Ye Y, Zhang Y, Lu X, Huang X, Zeng X, Lai X, et al. The anti-inflammatory effect of the SOCC
688 blocker SK&F 96365 on mouse lymphocytes after stimulation by Con A or PMA/ionomycin.
689 *Immunobiology* 2011;216:1044-1053.

690